Korean Journal of Remote Sensing, Vol.18, No.5, 2002, pp.273~279

Forward Mapping of Spaceborne SAR Image Coordinates to Earth Surface

Dong-Seok Shin and Won-Kyu Park

Image/System Divition, SaTReC Initiative Co. Ltd.

Abstract : This paper describes a mathematical model and its utilization algorithm for calculating the accurate target position on the ellipsoidal earth surface which corresponds to a range-azimuth coordinates of unprocessed synthetic aperture radar (SAR) images. A geometrical model which is a set of coordinate transformations is described. The side-looking directional angle (off-nadir angle) is determined in an iterative fashion by using the model and the accurate slant range which is calculated from the range sampling timing of the instrument. The algorithm can be applied not only for the geolocation of SAR images but also for the high quality SAR image generation by calculating accurate Doppler parameters.

Key Words : SAR, Forward Mapping, Range Gate, Doppler Centroid.

1. Introduction

The synthetic aperture radar (SAR), as a high resolution microwave earth observation payload providing earth surface information complementary and independent to that of optical payloads, has long been providing valuable information to remote sensing world wide. Its day-and-night operation as well as weather-free imaging capability highlights its usefulness over the spaceborne optical sensors.

It is well known that the accurate estimation of the expected phase histories of targets on the earth's surface are required for processing spaceborne SAR data in order to generate high quality images. In general, the phase history is characterized by the Doppler centroid and the Doppler frequency rate (Doppler parameters inclusively). The uncertainty of the estimated Doppler centroid leads to the loss of signal-to-noise ratio (SNR), the increase in ambiguity levels, and therefore, the degradation of image quality (Curlander and McDonough, 1991).

The Doppler parameters can be estimated systematically by using ancillary data (ephemeris and attitude data) of the spacecraft (Li *et al.*, 1985). When the ancillary data are not accurate enough, however, the parameters are estimated directly from the SAR raw signal data. The Doppler parameter estimation from the SAR data is known as clutter-lock (Doppler centroid) and auto-focus (Doppler rate). The image based parameter estimation techniques suffer not only from the additional computations but also from the errors due to noise and heterogeneous target reflectivity distribution. In addition, the results of the image based parameter estimation is generally validated by the results of the

Received 20 August 2002; Accepted 25 September 2002.

systematic parameter estimation when the ancillary data of a resonable accuracy is available. Therefore, the accurate systematic model for calculating Doppler parameters should be established in order to generate high-quality SAR images.

The camera model is the geometrical model which relates the pixel/line coordinates of an image and the coordinates on earth surface. The image to earth direction is generally referred as forward mapping and the earth to image direction is inverse mapping (Shin & Lee, 1997). In this term, this paper describes the forward mapping model and algorithm for SAR images.

The SAR imaging mechanism is intrinsically different from that of optical sensors. Its side-looking range-based scanning requires the conversion step between a slant range space and a ground range space. Moreover, the earth rotation should be included in the model since the Doppler frequency is based on the relative speed and acceleration of the platform and the earth surface (Wu *et al.*, 1982). Several papers have described on the systematic Doppler parameter estimation (Wu *et al.*, 1982; Li *et al.*, 1985). They are however based on the assumption that the target vector has already been derived.

This paper describes a method for deriving the target vector at the time of imaging and range scanning. The slant range is calculated by range bin coordinates and corresponding range gates (Section 2). An iterative algorithm (Section 4) and its intrinsic mapping model (Section 3) are used for deriving accurate target position corresponding to the image range/azimuth coordinates. Section 5 shows doppler centroid examples and range compressed image samples in the case of JERS-1 and ERS-2 SAR data.

During the model description in this paper, earth is modeled as an ellipsoid. The Earth Centered Inertial (ECI) coordinate space is chosen as the mapping reference frame in order for the further application such as Doppler parameter estimation. In this sense, the calculated target vector must be converted to Earth Centered of Rotation (ECR) in order to calculate geocentric or geodetic latitude and longitude.

2. Slant Range and Initial Off-Nadir Angle Calculation

The slant range is calculated from the range bin number which is generally equal to the pixel coordinate (column) of unprocessed SAR images. The timing diagram shown in Fig.1. describes the returned echo signal sampling mechanism of SAR.

SAR transmits a pulse repetitively with pulse repetition frequency (PRF) and samples the returned echo signal from the offset time (T_{off}) after the pulse transmission with the sampling frequency (f_{sf}). The on-board timing circuits control the offset time precisely according to the current position and orbital parameters. The offset time information is transmitted to a ground station for accurate timing analysis of a SAR processor (NASDA, 1991).

Since the two-way round trip time is generally greater than the pulse repetition interval, the sampled echo signal of i-th transmitted pulse is returned after the (i+N)-th transmitted pulse. For the platform of a near circular orbit, the N is fixed so that only T_{off} is controlled accurately. The period between the pulse transmission

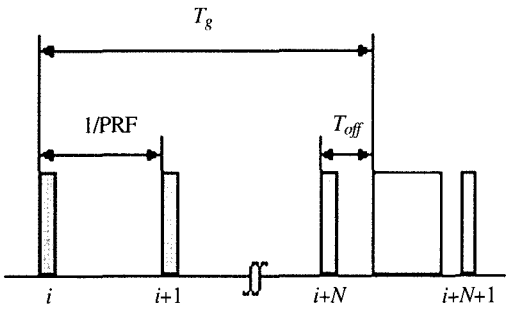

Fig.1. SAR echo sampling timing diagram.

and the returned echo sampling, which is called the range gate at early edge (T_g), is therefore,

$$T_g = T_{off} + \frac{N}{PRF}. \quad (1)$$

Since the echo signal is sampled with the sampling frequency in order to generate the in-phase and quadrature-phase data in the range direction, the round-trip time delay and hence the slant range R of the target corresponding to the range bin number r can be calculated as follows,

$$R = \frac{c\left(T_g + \frac{r}{f_{sr}}\right)}{2} \quad (2)$$

where c is the speed of light.

In order to generate the SAR forward mapping model the accurate look angle, so called off-nadir angle, must be determined. Since the accurate off-nadir angle for the ellipsoidal earth cannot be calculated directly from the slant range, the angle for the flat earth is calculated as an initial angle, so that it is refined by the iterative method which is described in the following sections.

The flat earth off-nadir angle, which is greater than the actual off-nadir angle with the ellipsoidal earth, can be calculated from the slant range R and the height of the satellite H which is provided in the ephemeris data:

$$\phi = \cos^{-1} + \left(\frac{H}{R}\right). \quad (3)$$

3. Forward Mapping Model

The model is basically a set of coordinate transformation from the sensor coordinate to the earth-centered coordinate. The forward mapping geometry model and its coordinate axes are illustrated in Fig. 2.

The basic rotational matrices which will be used in this and the next sections are defined as follows,

$$Rx(\theta) = \begin{pmatrix} 1 & 0 & 0 \\ 0 & \cos\theta & \sin\theta \\ 0 & -\sin\theta & \cos\theta \end{pmatrix}$$
$$Ry(\theta) = \begin{pmatrix} \cos\theta & 0 & -\sin\theta \\ 0 & 1 & 0 \\ \sin\theta & 0 & \cos\theta \end{pmatrix} \quad (4)$$
$$Rz(\theta) = \begin{pmatrix} \cos\theta & \sin\theta & 0 \\ -\sin\theta & \cos\theta & 0 \\ 0 & 0 & 1 \end{pmatrix}$$

The nadir pointing vector $P_1 = (0, 0, -1)$ in the sensor coordinate system is first transformed to P_2 in the platform coordinate system,

$$P_2 = Ry(\psi)P_1 \quad (5)$$

where ψ is off-nadir angle. The pointing vector is then transformed to P_3 in the orbit coordinate system which has its Z axis in the radial direction of the platform from the earth's center and its X axis in the orbit plane normal direction,

$$P_3 = Rx(\theta_p)Ry(\theta_r)Rz(\theta_y)P_2 \quad (6)$$

where θ_p, θ_r, θ_y are the pitch, roll and yaw angle of the satellite attitude respectively.

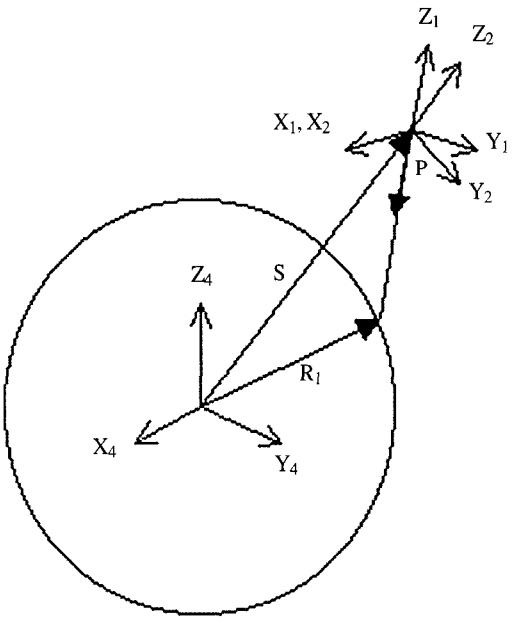

Fig. 2. Forward mapping geometry.

The pointing vector is transformed to the earth-centered coordinate system. Let $S = (S_x, S_y, S_z)$ and $V = (V_x, V_y, V_z)$ be the position and velocity vectors of the platform respectively in the earth-centered coordinate system and their normalized notations be S_{norm}, V_{norm}. The $Z = (z_1, z_2, z_3)$, $X = (x_1, x_2, x_3)$ and $Y = (y_1, y_2, y_3)$ axes of the orbit coordinate system in the earth-centered coordinate system can be obtained to be S_{norm}, $V_{norm} \times S_{norm}$, $Z \times X$, respectively according to the definition of the orbit coordinate system axes. The pointing vector in the earth-centered coordinate system, P_4, can be calculated by the directional matrix as follows,

$$P_4 = \begin{pmatrix} x_1 & y_1 & z_1 \\ x_2 & y_2 & z_2 \\ x_3 & y_3 & z_3 \end{pmatrix} \tag{7}$$

The pointing vector in the earth- centered coordinate system, $P_4 = (p_x, p_y, p_z)$, is projected to the ellipsoidal earth in order to obtain the target vector. The ellipsoidal earth and the pointing vector line from the platform can be represented in the Cartesian forms as follows,

$$\frac{(x^2 + y^2)}{R_e^2} + \frac{z^2}{R_p^2} = 1 \tag{8}$$

$$(x, y, z) = a(p_x, p_y, p_z) + (S_x, S_y, S_z)$$

where R_e and R_p are the semi-major and semi-minor axes of the earth ellipsoid respectively. The unknown variable a can be obtained by solving the second degree equations in Eq. (8):

$$a = \frac{-B - \sqrt{B^2 + AC}}{A}$$

$$A = (p_x^2 + p_y^2)R_e^2 + p_z^2 R_e^2 \tag{9}$$

$$B = (p_x S_x + p_y S_y)R_p^2 + p_z S_z R_e^2$$

$$C = (S_x^2 + S_y^2)R_p^2 + S_z^2 R_e^2 - R_e^2 R_p^2.$$

The target vector R_t is therefore,

$$R_t = aP_4 + S. \tag{10}$$

4. Iterative Estimation

In the forward mapping model which is described in the previous section, the only parameter which cannot be determined directly from the initial timing, ephemeris and attitude data is the off-nadir angle shown in Eq.(5). In this sense, an iterative algorithm must be used in order to obtain the accurate forward mapping results.

Firstly, the accurate slant range R and initial off-nadir angle ψ are obtained by the method described in Section 2. Then, the initial slant range a is calculated by the SAR forward mapping model, especially described in Eq.(10). Then, the off-nadir angle ψ must be updated (see following paragraphs) and the forward mapping model is applied iteratively until the difference between a and R is within a required precision. Using this algorithm, the iterative procedure of the forward mapping model converges within a couple of iterations.

The geometrical relationship between the slant range difference and the off-nadir angle difference is shown in Fig. 3. The off-nadir angle difference, which is the updating factor of the iterative algorithm can be calculated as follows,

$$\Delta\phi = \frac{a - R}{R \tan\phi} \tag{11}$$

where ϕ is the angle of incidence at the target.

In order to obtain the angle of incidence, the platform position vector in the earth-centered coordinate system

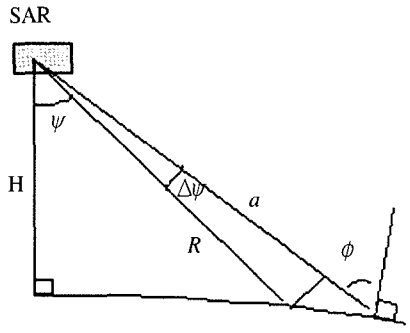

Fig. 3. Off-nadir angle difference geometry.

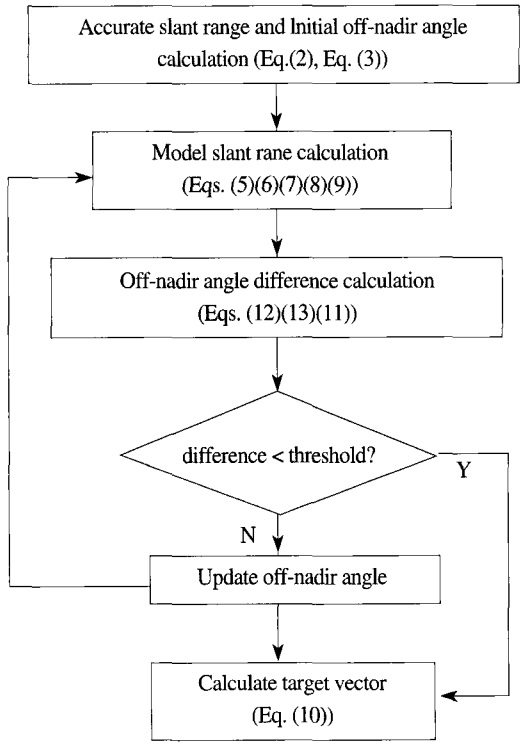

Fig. 4. Proposed algorithm flow.

is transformed to the horizontal reference coordinate system in which Z axis is normal to the target position on earth surface.

$$(x_h, y_h, z_h) = Ry(\frac{\pi}{2}-\omega)Rz(\lambda)(S-R_t) \quad (12)$$

where ω, λ is the geodetic latitude and longitude of R_t. The angle of incidence is therefore,

$$\phi = \sin^{-1}\left(\frac{z_h}{x_h}\right) \quad (13)$$

The overall flow of the proposed algorithm is described in Fig. 4.

5. Experiments

A JERS-1 SAR data and a ERS-2 SAR data (Table 1) were applied to the proposed algorithm in order for calculating Doppler centroid values corresponding to target positions on earth surface, which were derived from the proposed method.

Table 1. Experimental Images.

	JERS-1	ERS-2
center lat/long	37.7 / 126.7	63.9 / -145.6
acq. date	12 Aug 1998	25 Oct 1995
wavelength	23.513 cm	5.656 cm
sampling freq	17.076 MHz	18.959 MHz
PRF	1555.199 Hz	1679.902 Hz

The Doppler centroid (f_{DC}) is determined by the following equation (Madsen, 1989),

$$f_{DC} = -\frac{2(S-R_t)\cdot(V-V_t)}{\lambda\|(S-R_t)\|} \quad (14)$$

where λ is the wavelength of the SAR signal and S, V are the position, velocity vector of the platform in the earth-centered coordinate system, respectively. The position and velocity of the platform can be obtained from the ephemeris record of the raw signal data. R_t and V_t are the position and the velocity of the target on earth's surface, which are obtained by the proposed algorithm.

Fig. 5 shows the Doppler centroid variation along the azimuth and the range directions. While the JERS-1 data shows large Doppler centroid values (~2000Hz) as well as a large variation (~200Hz), the Doppler centroid of the ERS-2 data shows small absolute values (~200Hz) and variation (~20Hz). This is due to the fact that ERS-2 provides a continuous yaw-steering control with respect to the earth's rotation velocity, so that the relative Doppler shift is minimized. Since the ERS-2 data contains only one attitude information sample, the continuous yaw steering mechanism was not applied to the Doppler shift variation in the azimuth direction. If several attitude information samples were provided, the yaw-steering mechanism could be applied by the attitude sample interpolation, and hence, the Doppler centroid variation in the azimuth direction became even smaller.

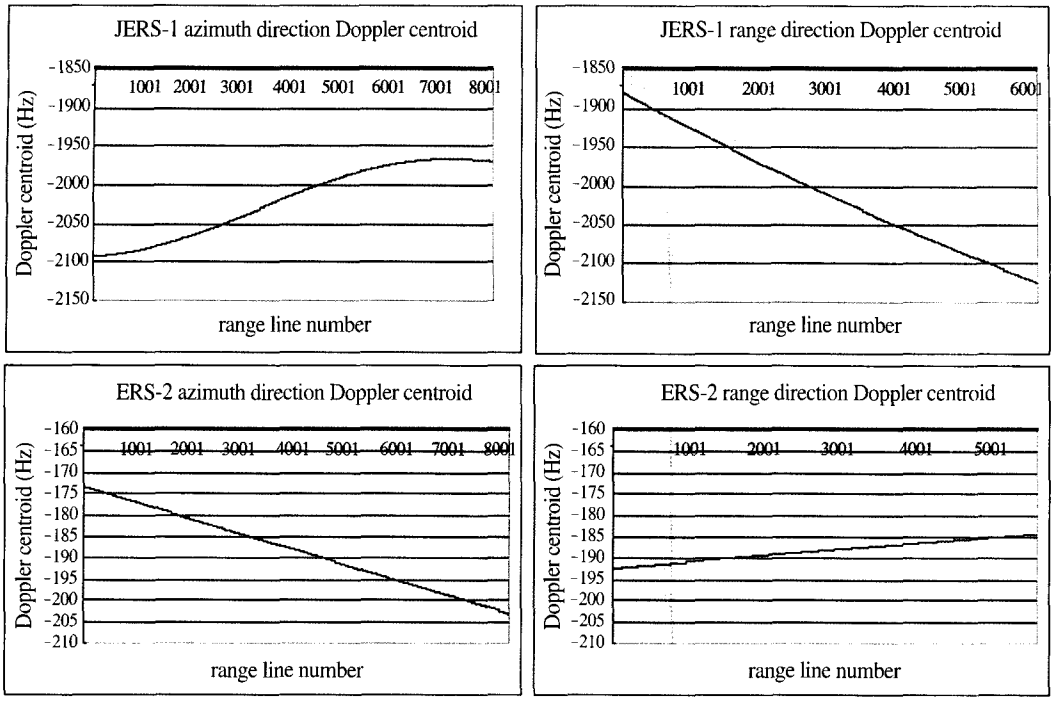

Fig. 5. Doppler centroid variation along azimuth and range direction.

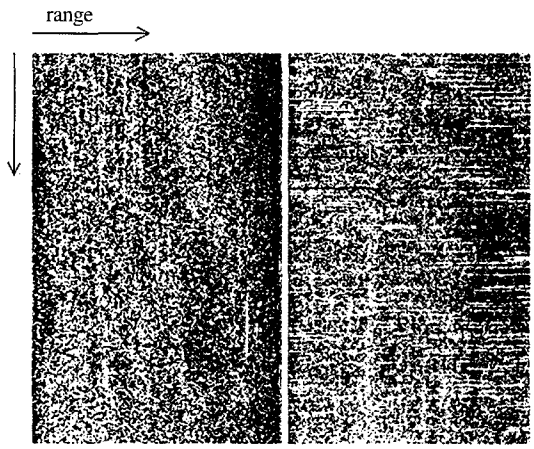

Fig. 6. Range compressed image : ERS-2 (left) and JERS-1 (right).

Fig. 6 shows the range compressed image data. It can be seen that JERS-1 range compressed image shows a large range skew because of the large value of the Doppler centroid and its variation. This skew or curvature in the range direction can be corrected by a range migration correction technique. The horizontal stripes and low quality shown in the JERS-1 range compressed image is due to the unstable power supply of the JERS-1 and its low data quantization levels (3-bits), respectively.

6. Conclusions

In this paper we described a SAR forward mapping model from the range bin number and the ephemeris/attitude information of the platform. In addition, an iterative method for utilizing the forward mapping model is also described. The proposed model does not use any approximation and hence its accuracy depends only on the accuracy of a priori information (e.g. position, velocity, attitude of the platform as well as

the SAR sensor parameters). In order to show one of the potential applications, the model and algorithm was applied for calculating Doppler centroid values of JERS-1 and ERS-2 raw data. The algorithm can also be applied for precise geolocation of SAR images as well as deriving the Doppler parameters and hence the accurate phase history as a spaceborne SAR scans the targets on earth surface along the range and azimuth direction.

References

Curlander, J.C. and R.N. McDonough, 1991. *Synthetic Aperture Radar Systems and Signal Processing*, John Wiley & Sons Inc., New York.

Li, F.K., D.N. Held, J.C. Curlander and C. Wu, 1985. Doppler Parameter Estimation for Spaceborne Synthetic Aperture Radars, *IEEE Trans. Geoscience and Remote Sensing*, GE-23(1): 47-56.

Madsen, S.N., 1989. Estimating the Doppler Centroid of SAR Data, *IEEE Trans. Aerospace and Electronic Systems*, AES-25(2): 134-140.

NASDA, 1991. *JERS-1 to Ground Station Interface Description*, HE88023, rev.3, EOC/NASDA.

Shin, D. and Y.R. Lee, 1997. Geometric Modelling and Coordinate Transformation of Satellite-Based Linear Pushbroom-Type CCD Camera Images, *J. Korean Society of Remote Sensing*, 13(2): 85-98.

Wu, C., K.Y. Liu and M. Jin, 1982. Modeling and a Correlation Algorithm for Spaceborne SAR Signals, *IEEE Trans. Aerospace and Electronic Systems*, 18(5): 563-575.